Ocean Sci. Discuss., doi:10.5194/os-2016-106, 2017
Manuscript under review for journal Ocean Sci.
Published: 9 January 2017

Ocean Science
Discussions
Open Access
EGU

Medium-term dynamics of a Middle Adriatic barred beach

Matteo Postacchini[1], Luciano Soldini[1], Carlo Lorenzoni[1], and Alessandro Mancinelli[1]
[1]Department of Civil and Building Engineering, and Architecture, Università Politecnica delle Marche, 60131 Ancona, Italy
Correspondence to: Matteo Postacchini (m.postacchini@univpm.it)

Abstract. In the recent years, attention has been paid to beach protection by means of soft and hard defenses. Along the Italian coasts of the Adriatic Sea, sandy beaches are the most common landscapes and around 70 % of the Marche-Region coasts (central Adriatic), is protected by defense structures. The longest free-from-obstacle nearshore area in the region includes the beach of Senigallia, characterized by a multiple barred beach, frequently monitored during the last decades. The bathymetries surveyed in 2006, 2010, 2011, 2012 and 2013 show long-term stability, confirmed by a good adaptation of an analyzed stretch of the beach to the Dean-type equilibrium profile, though a strong short-/medium-term variability of the wave climate has been observed during the monitored periods. This suggests a slight influence of wave forcing on the long-term profiles, which seems to only depend on the sediment size. Further, the medium-term dynamics of the submerged bars and their geometric features have been related to the wave climate collected, during the analyzed temporal windows, by a wave buoy located 40 km off Senigallia. An overall interpretation of the complete dynamics, i.e. hydrodynamics (buoy data), sediment characteristics (equilibrium-profile A parameter) and morphodynamics (bathymetric surveys), suggests that the wave climate is fundamental for the morphodynamic changes of the beach in the medium term: waves coming from NNE/ESE, characterized by a larger/smaller steepness and by a larger/smaller relative wave height, induce seaward/shoreward bar migration, as well as bar smoothing/steepening. Moving southeastward, the bar dimension increases, while the equilibrium profile shape suggests the adaptation to a decreasing sediment size in the submerged beach. This is probably due to the presence of both the harbor jetty and river mouth North of the investigated area.

1 Introduction

Our communities are experiencing a series of problems and difficulties related to the inundation risk in the coastal areas, the protection of nearshore regions, the use of beaches for tourist and recreational activities. In the last decades, an increasing attention has been paid to short- and long-term predictions associated with the climate change, which is strictly related to the above-mentioned aspects (e.g., see Houghton et al., 2010; Ranasinghe et al., 2013). In fact, such predictions are associated with both the mean sea-level rise and the more frequent sea storms, also occurring during the summertime. The understanding of the main physical processes driven by such changes is fundamental for (i) the modeling of the nearshore dynamics, also in terms of rapid morphological changes of the beach (e.g., Postacchini et al., 2016b), (ii) the correct prediction of coastal flooding (e.g., Villatoro et al., 2014), and (iii) the proper design of protection solutions (e.g., Lorenzoni et al., 2016).

Ocean Sci. Discuss., doi:10.5194/os-2016-106, 2017
Manuscript under review for journal Ocean Sci.
Published: 9 January 2017

Several studies (e.g., Benavente et al., 2006; Walton and Dean, 2007) showed that a proper representation of the local bathymetry is fundamental both to correctly predict the seabed changes induced by wave/current forcing and to design efficient solutions for the coastal protection. Hence, typical bedforms of unprotected sandy beaches should be taken into due account. In particular, submerged subtidal bars usually form on bottom slopes within 0.005–0.03 and their height ranges between some centimeters to meters (Leont'ev, 2011). In semi-protected and open coasts, two-dimensional longshore bars are quite common and have been extensively studied, though the complex mechanisms of generation and migration are not yet completely understood. Generation of submerged bars can be ascribed to three different mechanisms, i.e. wave breaking, infragravity waves and self arrangement (Wijnberg and Kroon, 2002), while the bar migration depends on several coastal processes and has been investigated both in the field (e.g., Ruessink et al., 1998), numerically (e.g., Dubarbier et al., 2015) and through laboratory experiments (e.g., Alsina et al., 2016). It has been observed that swash-zone slope, grain size and wave characteristics play an important role. The influence of the former on the bar dynamics has only been observed during laboratory experiences, after an ad hoc manual reshaping of the swash zone (Baldock et al., 2007; Alsina et al., 2012). On the other hand, field observations confirmed that the grain size could be important in the bar migration rates, due to the larger sediment transport induced by finer sands (Goulart and Calliari, 2013), while the wave characteristics are fundamental for the bar migration direction. In particular, the wave breaking over the bars leads to the generation of a deep return flux, known as undertow, which promotes a seaward motion. As an example, Gallagher et al. (1998) observed, near Duck (North Carolina), an intensified wave breaking occurring over the bar during storms, this inducing a large undertow inshore of the bar that pushed it seaward. Conversely, a shoreward bar migration was also observed under small waves, during less energetic states (see also Goulart and Calliari, 2013).

While numerical simulations well reproduced the offshore migration during severe conditions, some difficulties arose when reproducing the onshore bar motion during mild wave conditions (Gallagher et al., 1998; Plant et al., 2004), this suggesting that not all the processes involved in the bar migration were clearly understood and correctly simulated, e.g., lower-frequency waves. Further, Ruessink et al. (1998), who analyzed the cross-shore sediment transport and morphological changes occurring in the nearshore area of Terschelling (Netherlands), stated that the role of the infragravity waves have not been completely understood. In particular, it was fairly clear that during energetic conditions, the suspended load dominated over the bedload and the morphodynamics were controlled by undertow, and, probably, infragravity waves: the latter, more important during breaking than during calm conditions, mobilize large amounts of sediments, which are then advected offshore by the undertow.

The importance of infragravity waves is confirmed by other authors, and a detailed study about their influence on the bar dynamics was undertaken by Aagaard et al. (1994) using field data collected at Stanhope Lane Beach (Canada). They stated that the sediment transport induced by infragravity waves may be either shoreward or seaward, and suspended sediments are mainly transported towards antinodes in the water surface elevation. However, the contribution of infragravity waves on both sediment transport and sandbar motion can be neglected on time scales of years, i.e. when dealing with medium-term morphodynamics (Ruessink and Terwindt, 2000).

With the purpose to characterize the sandbar migration, an important parameter has been recently introduced. This is the local relative wave height, i.e. the ratio between local wave height H and water depth over the bar crest h_{cr}. Values smaller than ~ 0.3 promote landward migration, while values larger than 0.6 promote seaward migration (Houser and Greenwood, 2005).

Ocean Sci. Discuss., doi:10.5194/os-2016-106, 2017
Manuscript under review for journal Ocean Sci.
Published: 9 January 2017

In particular, along the Dutch coast (Ruessink et al., 1998; Ruessink and Terwindt, 2000), a relative wave height $H_s/h_{\rm cr} = 0.33$ represented the onset of breaking, with H_s being the local significant height. Hence, $H_s/h_{\rm cr} > 0.33$ referred to breaking intensification and undertow increase, leading to seaward bar migration. While $H_s/h_{\rm cr} < 0.33$ indicated dominance of short waves and wave skewness, leading to shoreward bar migration. The analysis of the velocity moments and sediment transport confirmed the correlation between medium-term wave conditions and short-term sediment transport measurements (Ruessink and Terwindt, 2000).

From a physical point of view, the increase of both $H_s/h_{\rm cr}$ and breaking intensification produces an increase of the breaking wave celerity (e.g., see Postacchini and Brocchini, 2014), this leading to an intensification of the shoreward volume flux, hence to a wave setup (e.g., see Soldini et al., 2009) and to the following increase of the undertow velocity (e.g., see Kuriyama and Nakatsukasa, 2000).

Only few literature studies have been carried out to investigate the seasonal and annual scale of the beach dynamics (e.g., Ruggiero et al., 2009). Some field observations confirmed a cyclic behavior of multiple bars (Ruessink and Terwindt, 2000; Goulart and Calliari, 2013), mainly characterized by three stages, i.e. initial generation, seaward migration and final degradation. Conversely, other authors observed a continuous landward motion, until bar-shore welding, even during storm events (Aagaard et al., 2004). While the offshore migration is promoted by the undertow dominance in the net transport balance, as already stated, the onshore migration is probably enhanced by storm surge. In fact, the surge (i) increases both skewness and phase coupling, and (ii) reduces the undertow contribution.

The present study describes the seabed evolution of a natural unprotected beach stretch of Senigallia (Marche Region, Italy), a touristic town of the Italian Middle Adriatic. The available bathymetries, covering the last decade, and the wave climate, enable us to analyze the medium-term morphological evolution of the beach, including the geometry and migration of the submerged bars, as a function of the wave forcing. To the authors' knowledge, this is the first study on the medium-term beach evolution and bar migration occurring in a sandy beach of the Adriatic Sea, a semi-enclosed basin characterized by small tidal excursions (40cm) and reduced wave heights, if compared to the above-mentioned coastal areas.

The manuscript is divided as follows. Sect. 2 and Sect. 3 illustrate, respectively, the investigated site and the available data. Results are presented in Sect. 4 and discussed in Sect. 5. Some conclusions close the paper.

2 Description of the site

The analyzed coast is part of the longest unprotected beach of the Marche Region, which extends from the estuary of the Misa River, whose final reach is highly engineered and adjacent to the Senigallia harbor, to $\sim 3.5\,{\rm km}$ North of the Esino River estuary, hence for a total length of $\sim 12\,{\rm km}$ (Fig. 1). As observed during recent field experiments, the coastal region around the Misa River estuary is dynamic throughout the year, especially during sea storms driven by NNE winds, which mobilize a large amount of sediment and generate significant erosion/deposition patterns nearby the rigid structures (Brocchini et al., 2015, 2016). The investigated site is characterized by a swash-zone slope in the range $1:30$–$1:40$, an array of submerged bars in a water depth $h = 0$–$3\,{\rm m}$, and a mild slope of about $1:200$ for $h > 3\,{\rm m}$ (example of cross-shore profiles are illustrated in

Ocean Sci. Discuss., doi:10.5194/os-2016-106, 2017
Manuscript under review for journal Ocean Sci.
Published: 9 January 2017

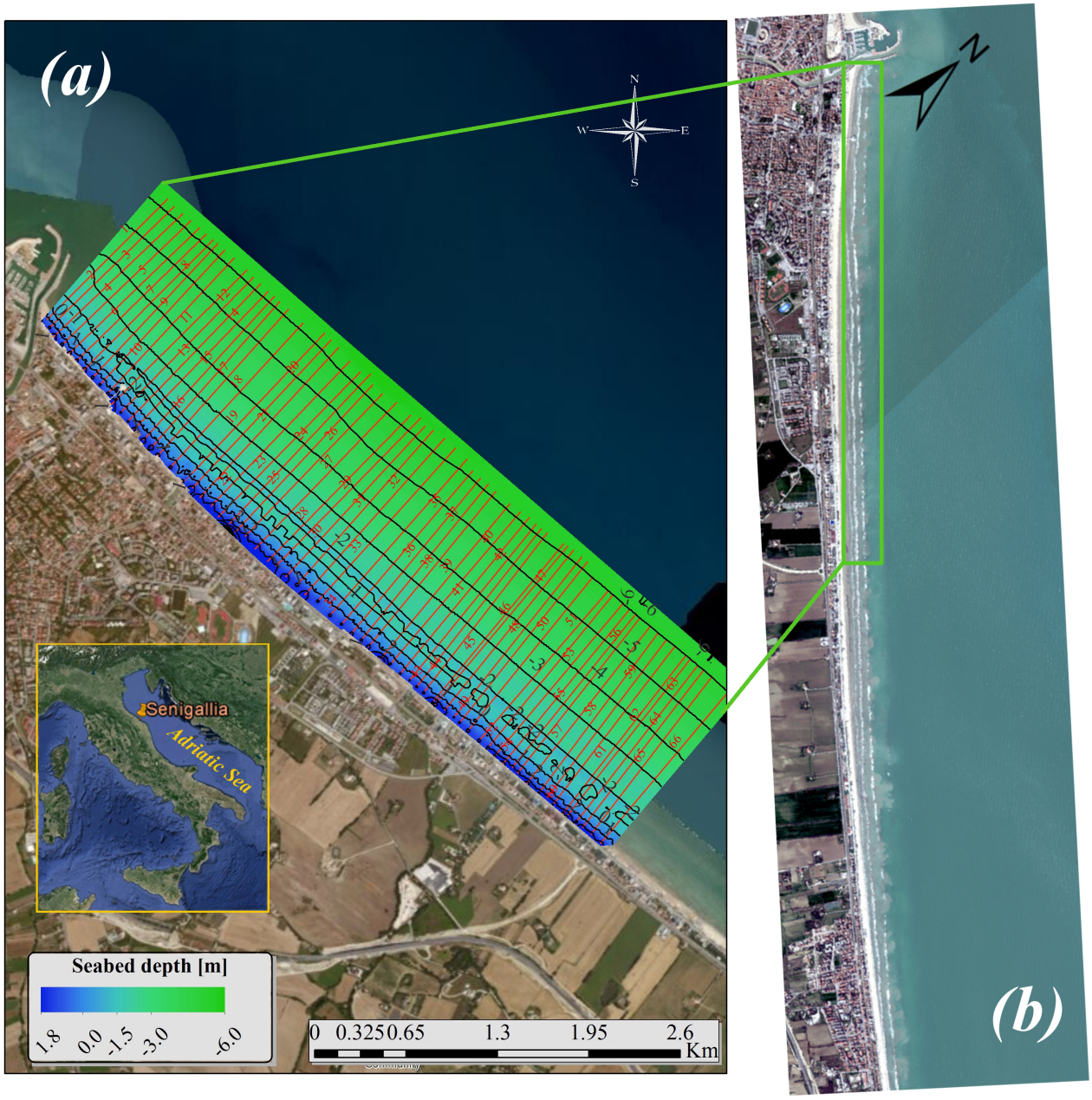

Figure 1. Natural beach of Senigallia: **(a)** bathymetry with isobaths and position of cross-shore profiles referring to June 2006 (the white spot between profiles 11 and 12 is the "Rotonda") and **(b)** satellite view of $\sim 10\,\mathrm{km}$ beach South of the harbor/Misa River estuary.

Ocean Sci. Discuss., doi:10.5194/os-2016-106, 2017
Manuscript under review for journal Ocean Sci.
Published: 9 January 2017

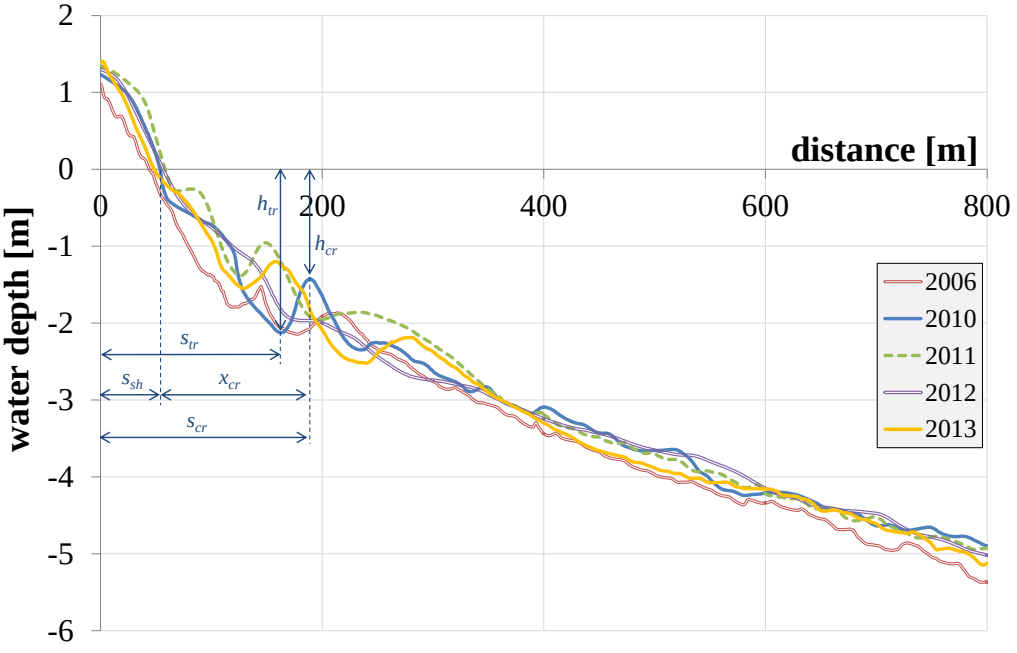

Figure 2. Example of cross-shore profile evolution during the investigated years. Bar characteristics referring to the 2010 profile are also reported.

Fig. 2). The emerged beach is characterized by fine ($d_{50} = 0.125$–$0.25\,\mathrm{mm}$) and medium ($d_{50} = 0.25$–$0.5\,\mathrm{mm}$) sands, while fine sand was found in the submerged part.

The wave climate in the investigated area was obtained from a waverider of the Italian wave measurement network (RON), located $\sim 23\,\mathrm{nm}$ East-North-East of Senigallia. It worked between March 1999 and March 2006 and between December 2009 and November 2013, the data between 2006 and 2010 surveys thus missing. During the 11 years recordings, the waves mainly came from ESE and NNE (Fig. 3a), the main events hence induced by Bora (coming from NNE) and Levante-Scirocco (from ESE) winds. The wave frequency (blue outline) is better distributed throughout the directions, while the wave energy (orange area) is characterized by sharper peaks corresponding to ESE and NNE.

The analysis of the beach morphology, using the concept of the equilibrium beach profile, leads to the estimate of both the so-called "fitting depth" and the shape parameter A, which strictly depends on d_{50}, for each single cross-shore profile (e.g., Walton and Dean, 2007). See also the discussion in Sect. 5.

Ocean Sci. Discuss., doi:10.5194/os-2016-106, 2017
Manuscript under review for journal Ocean Sci.
Published: 9 January 2017

The submerged beach, surveyed in 2006, 2010, 2011, 2012 and 2013 up to a depth of $\cong 6m$ (see also Sect.3), has been extended up to $10m$ assuming as constant the mild slope characterizing the deeper beach stretch, i.e. $1:200$, in order to estimate a proper fitting depth. Using either the least-square approach or the continuity of volume, i.e. integration of Eq. (4), the results are similar. From the DTM of Fig. 1a, referring to the 2006 survey, 66 profiles have been extracted. It is important to notice that A, and similarly d_{50}, decreases moving southward. The largest values occur close to the Senigallia harbor (profile 1 of Fig. 1a), i.e. $A \cong 0.069$ and, following Hanson and Kraus (1989), $d_{50} \cong 0.15\,\mathrm{mm}$, while the smallest occur $\sim 3.9\,\mathrm{km}$ South of the harbor (profile 66), where $A \cong 0.060$ and $d_{50} \cong 0.13\,\mathrm{mm}$. Such values are in agreement with the fine sand characterizing the submerged beach (Lorenzoni et al., 1998a). It has been observed that, throughout the coast surveyed in 2006, the natural beach well adapts to the Dean-type equilibrium profile. This is confirmed by the following campaigns (2010–2013), when a good adaptation still exists, the values of A remain almost constant in time and decrease moving southward. Further, the fitting depth increases from the harbor to the "Rotonda", i.e. the pile-mounted permeable structure within profiles 11 and 12, and decreases South of the "Rotonda". This suggests a sediment motion occurring at larger depths in correspondence of the structure, that partially (and locally) influences the beach evolution and bar migration.

3 Experimental data

The natural beach of Senigallia was characterized by a number of bathymetric surveys since the 80s. More recently, due to a specific requirement of the Marche Region, a detailed survey of the nearshore region of Senigallia was undertaken in June 2006, both North and South of the harbor, such areas being respectively characterized by a protected and an unprotected beach. The surveys cover the nearshore region up to a depth of $6\,\mathrm{m}$ and a total length of $4.3\,\mathrm{km}$, most of which ($\sim 3.9\,\mathrm{km}$) South of the harbor (Fig. 1a).

Between 2010 and 2013, after the modification of the harbor entrance, annual bathymetric surveys up to a depth of $6\,\mathrm{m}$ were carried out by the municipality of Senigallia on a $2.5\,\mathrm{km}$-long area covering part of the protected and part of the unprotected beaches.

The analysis of the available surveys enabled us to extract 18 cross-shore profiles which characterize the unprotected beach for about $1\,\mathrm{km}$. This is used for the analysis of the morphological changes induced by the wave climate throughout years, in terms of bar migration and geometry.

From the analysis of both surveys and satellite data, the submerged bars remain for a stretch of $\sim 12\,\mathrm{km}$. Further, moving southeastward, the sediment size changes, with a transition from sand to gravel occurring $\sim 6\,\mathrm{km}$ South of the harbor (Lorenzoni et al., 1998b). Hence, the initially two-dimensional longshore bars of the investigated area get closer to the shoreline, thus switching to three-dimensional (see Fig. 1b, where the location of the bars is highlighted by both foam and suspended sediment induced by the waves breaking over them). However, the $\sim 1\,\mathrm{km}$-long area South of the harbor can be taken as representative of the sandy beaches characterizing the Middle Adriatic Sea and will be analyzed in the next sections.

Ocean Sci. Discuss., doi:10.5194/os-2016-106, 2017
Manuscript under review for journal Ocean Sci.
Published: 9 January 2017

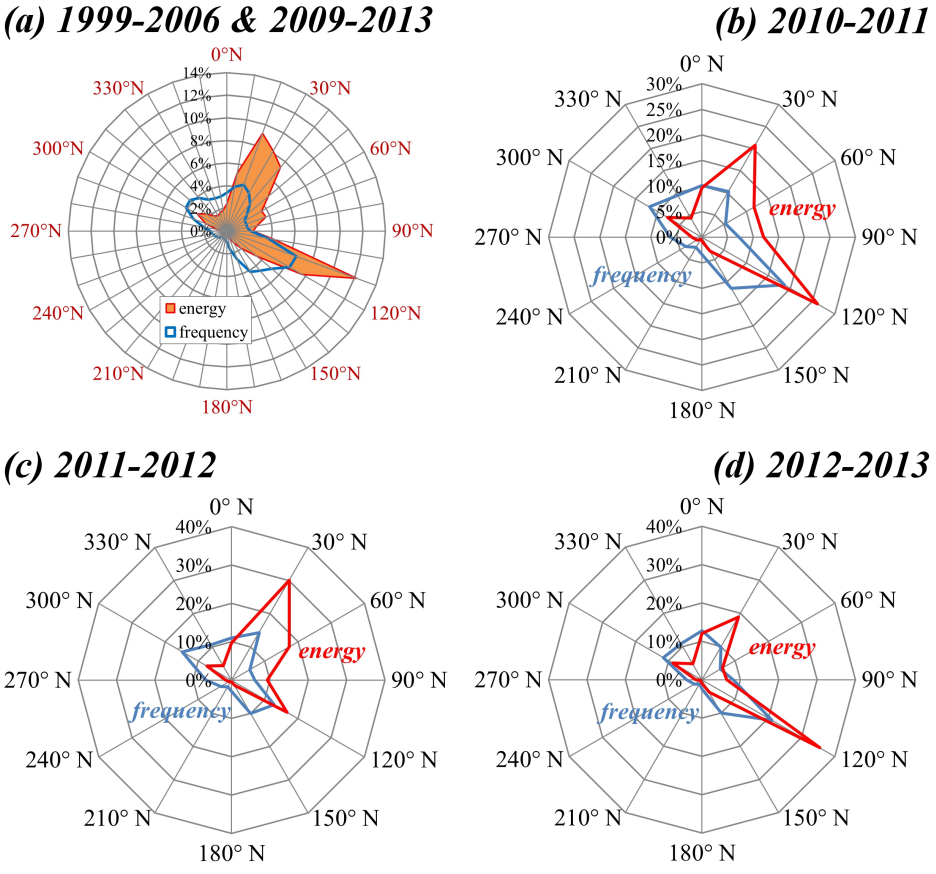

Figure 3. Wind roses of wave energy (red line) and frequency (blue line) referring to time periods: **(a)** 1999–2006 and 2009–2013, **(b)** 2010–2011, **(c)** 2011–2012 and **(d)** 2012–2013..

4 Results

The following sections illustrate the results obtained from the analysis of the seabed variation using the available bathymetric surveys, which refer to June 2006, February 2010, February 2011, April 2012 and May 2013, and the related wave climate. Both migration and geometry of the submerged bars are also discussed.

4.1 Wave climate

Except for the period 2006–2010, during which the waverider did not work, the wave climate referring to the considered time periods is illustrated in Fig. 3: both the overall climate (Fig. 3a) and the single-period climates (2010–2011 in Fig. 3b; 2011–2012 in Fig. 3c; 2012–2013 in Fig. 3d) are shown. The most frequent and the most energetic waves are, in both cases, those coming from either ESE, i.e. forced by Levante-Scirocco winds, or NNE, i.e. forced by Bora winds, which thus correspond to the predominant waves of such a coastal area. While the wave frequency (blue lines), though the NNE and ESE peaks, results

Ocean Sci. Discuss., doi:10.5194/os-2016-106, 2017
Manuscript under review for journal Ocean Sci.
Published: 9 January 2017

fairly well distributed and homogeneous if the different roses are compared, the wave energy (red lines) is characterized by sharper peaks in correspondence of these dominant directions and by a reduced distribution elsewhere. It is worth noting that directions of yearly dominant waves result variable.

It is well known that the wave climate for the extra-tropical regions at intermediate latitudes, like that of the Adriatic Sea, is characterized by the presence, at the soil level, of closed dynamical systems, as cyclones and anticyclones. Usually, soil weather systems are connected to a movement with an upper-level wavy structure, that slowly migrates eastward. So, the presence of migrating temporal troughs and ridges alternates during the year. Troughs are linked to low atmospheric pressure areas, with colder air and a sequence, usually, of cyclones. Ridges are linked to high pressure areas, with warmer air and anticyclonic, more stable, weather.

Hence, the weather is not characterized by two distinct (seasonal) behaviors: the two peaks illustrated in the single panels of Fig. 3 do not refer to the prevalent conditions occurring, respectively, e.g., in summer and winter, but mainly refer to the most severe winter storms, the summertime being characterized by milder wave conditions, due to less strong winds and slowly changing wind directions during storms (see also Brocchini et al., 2015). The alternation in the winter-storm direction, which remains almost constant during the storm growth, is confirmed by Brocchini et al. (2016), who observed two consecutive storms, the first due to Bora wind and the second, after three days, due to winds coming from WNW and N. The dominance of one peak on the other underlines the pronounced temporal variability of the wave climate during the year (especially in winter), with some years (or winters) characterized by a larger number of Scirocco than Bora storms, and vice-versa. The fairly well distributed frequency, with respect to the more peaked energy flux (Fig. 3), indicates that the annual variability of storms is not bound to the seasonal variability of wave climate.

Further, the Bora is a cold and dry wind usually linked to a well-developed anticyclone on the central or northern Europe and a relative low pressure on the Mediterranean Sea. It is more frequent and very intense during the winter. Conversely, the Scirocco is a southern warm wind, which is dry in Africa, then becomes wet passing on the Mediterranean Sea, and finally generates big sea storms with important surges and persistent swell. Scirocco intensities are less than the Bora, but generate longer and more enduring waves.

With reference to both frequency and energy flux, a statistic analysis of the main sectors has been undertaken for each selected time period, i.e. ESE sector (105–135°) for 2010–2011 and 2012–2013, and NNE sector (15–45°) for 2011–2012. During the former time periods, the largest energetic contribution is ascribed to significant wave heights in the range $H_{\mathrm{m0}} = (1\text{–}3)\,\mathrm{m}$ (2010–2011) and $H_{\mathrm{m0}} = (1.5\text{–}3.5)\,\mathrm{m}$ (2012–2013). The most frequent waves falling in such ranges are characterized by mean periods $T_{\mathrm{m}} = (4.5\text{–}6)\,\mathrm{s}$ (2010–2011) and $T_{\mathrm{m}} = (5\text{–}6.5)\,\mathrm{s}$ (2012–2013). In the same years, peak periods are respectively $T_{\mathrm{p}} = (6.5\text{–}8.5)\,\mathrm{s}$ and $T_{\mathrm{p}} = (7\text{–}8.5)\,\mathrm{s}$. In the period dominated by NNE waves, the largest energetic contribution belongs to a narrower wave-height range, i.e. $H_{\mathrm{m0}} = (1.5\text{–}2.5)\,\mathrm{m}$, which corresponds to most frequent waves falling within the ranges $T_{\mathrm{m}} = (4.5\text{–}5.5)\,\mathrm{s}$ and $T_{\mathrm{p}} = (6\text{–}7)\,\mathrm{s}$. The above-described procedure can be better understood observing Tab. 1, which illustrates the energy flux distribution within sector 105–135° for the time period 2010–2011, and Tab. 2, which refers to the corresponding frequency distributions for fixed ranges of H_{m0} and T_{m}.

Ocean Sci. Discuss., doi:10.5194/os-2016-106, 2017
Manuscript under review for journal Ocean Sci.
Published: 9 January 2017

Table 1. Energy-flux distribution (%) in 2010–2011 (only referring to sector 105–135°).

H_{m0} [m]										
0.0–0.5	0.5–1.0	1.0–1.5	**1.5–2.0**	2.0–2.5	2.5–3.0	3.0–3.5	3.5–4.0	4.0–4.5	4.5–5.0	>5.0
0.00	0.00	10.41	**16.56**	12.37	15.03	16.02	10.87	5.43	9.85	3.45

Table 2. Frequency (%) for classes of H_{m0} and T_m in 2010–2011 (only referring to sector 105–135°).

	H_{m0} [m]										
T_m [s]	0.0–0.5	0.5–1.0	1.0–1.5	**1.5–2.0**	2.0–2.5	2.5–3.0	3.0–3.5	3.5–4.0	4.0–4.5	4.5–5.0	>5.0
<2.00	0.00	0.00	0.00	0.00	0.00	0.00	0.00	0.00	0.00	0.00	0.00
2.0–2.5	0.00	0.00	0.00	0.00	0.00	0.00	0.00	0.00	0.00	0.00	0.00
2.5–3.0	0.00	0.00	0.00	0.00	0.00	0.00	0.00	0.00	0.00	0.00	0.00
3.0–3.5	0.00	0.00	0.56	0.00	0.00	0.00	0.00	0.00	0.00	0.00	0.00
3.5–4.0	0.00	0.00	7.61	0.00	0.00	0.00	0.00	0.00	0.00	0.00	0.00
4.0–4.5	0.00	0.00	11.86	1.90	0.00	0.00	0.00	0.00	0.00	0.00	0.00
4.5–5.0	0.00	0.00	9.40	7.72	0.56	0.00	0.00	0.00	0.00	0.00	0.00
5.0–5.5	0.00	0.00	8.39	**10.51**	3.47	0.78	0.00	0.00	0.00	0.00	0.00
5.5–6.0	0.00	0.00	2.13	6.82	4.59	2.80	0.45	0.00	0.00	0.00	0.00
6.0–6.5	0.00	0.00	0.00	1.01	2.80	3.02	2.68	1.12	0.00	0.00	0.00
6.5–7.0	0.00	0.00	0.00	0.00	0.00	1.79	2.01	0.78	0.45	0.11	0.00
7.0–7.5	0.00	0.00	0.00	0.00	0.00	0.00	1.01	1.12	0.22	0.89	0.22
7.5–8.0	0.00	0.00	0.00	0.00	0.00	0.00	0.00	0.00	0.45	0.56	0.22
8.0–8.5	0.00	0.00	0.00	0.00	0.00	0.00	0.00	0.00	0.00	0.00	0.00
8.5–9.0	0.00	0.00	0.00	0.00	0.00	0.00	0.00	0.00	0.00	0.00	0.00
9.0–9.5	0.00	0.00	0.00	0.00	0.00	0.00	0.00	0.00	0.00	0.00	0.00
9.5–10.0	0.00	0.00	0.00	0.00	0.00	0.00	0.00	0.00	0.00	0.00	0.00
>10.0	0.00	0.00	0.00	0.00	0.00	0.00	0.00	0.00	0.00	0.00	0.00

With the purpose of characterizing each time period with specific wave features, the most energetic direction (ESE/NNE), associated with the most probable wave-height range (e.g., $H_{m0} = 1.5$–2.0 in the example of Tab. 1), gives the most probable wave-period range (e.g., $T_m = 5.0$–5.5 in Tab. 2). This results in the following mean values, which represent the most probable combinations (H_{m0}, T_m) and (H_{m0}, T_p), related to the most energetic waves.

- 2010–2011: ESE, $H_{m0} = 1.75\,\mathrm{m}$, $T_m = 5.25\,\mathrm{s}$, $T_p = 7.25\,\mathrm{s}$
- 2011–2012: NNE, $H_{m0} = 2.25\,\mathrm{m}$, $T_m = 5.25\,\mathrm{s}$, $T_p = 6.75\,\mathrm{s}$
- 2012–2013: ESE, $H_{m0} = 1.75\,\mathrm{m}$, $T_m = 5.25\,\mathrm{s}$, $T_p = 7.25\,\mathrm{s}$

Ocean Sci. Discuss., doi:10.5194/os-2016-106, 2017
Manuscript under review for journal Ocean Sci.
Published: 9 January 2017

As expected, due to the available fetch length (see also Fig. 1a), a larger wave steepness ($H_{\mathrm{m0}}/L_{\mathrm{p0}}$, where L_{p0} is the deep-water peak wavelength) occurs during the NNE-dominated than during the ESE-dominated periods.

4.2 Bathymetric surveys

The available bathymetries have been overlapped using ArcGIS software and the difference in the bed depth has been estimated between each pair of consecutive surveys. Hence, Fig. 4 illustrates the difference between the bed depth measured in 2010 and that measured in 2006 (a), 2011 and 2010 (b), 2012 and 2011 (c), 2013 and 2012 (d). Each case shows seabed patterns which are mostly parallel to the coast. Such parallel patterns illustrate the different location of the submerged bars and their migration through years. In each panel, positive/negative values mean that a seabed accretion/erosion occurred during the considered time period. Large positive values indicate either the filling of the bar trough or the location of the bar crest at the end of the time period (e.g., see the longshore distribution of positive values in Fig. 4a, b, and d, these representing the crest location in 2010, 2011, 2013, respectively). Further, large negative values may also indicate a bar-crest smoothing and a general beach flattening, as shown in Fig. 4c. Notice that the largest variations occur in the nearshore area, i.e. for bed depths smaller than $3m$.

The shoreline is fairly stable and, in the medium-term, oscillates in the cross-shore direction less than $20\,\mathrm{m}$, with the largest motions occurring in 2006–2010 (advance) and 2011–2012 (retreat). To properly reconstruct the bar migration, the crest locations are overlapped to the color maps of Fig. 4.

Further, each of the 18 cross-shore profiles have been characterized by means of (also refer to Fig. 2): (i) the shoreline position from a fixed point (s_{sh}), (ii) the distance of each bar crest from both fixed point (s_{cr}) and shoreline ($x_{\mathrm{cr}} = s_{\mathrm{cr}} - s_{\mathrm{sh}}$), and (iii) the bar geometry, i.e. crest (h_{cr}) and trough (h_{tr}) depths. The location of both bar crest s_{cr} ($\square$ for the middle bar, $\circ$ for the outer bar) and shoreline s_{sh} ($\diamond$) are illustrated in Fig. 5a. A shoreward migration of the bars occurred in 2006–2010, 2010–2011 and 2012–2013, while a seaward motion only occurred between 2011 and 2012, when the bars were partially destroyed. After 2012, a partial bar regeneration occurred. The "Rotonda" (profiles 11–12) also affects the bar generation/existence, e.g. in 2010 the outer bar exists only South of the structure, in 2011 only North.

The influence of the permeable structure is also evident from the inspection of the ratio between trough and crest depths $h_{\mathrm{tr}}/h_{\mathrm{cr}}$ (Fig. 5b). The middle bars ($\square$) show almost regular, slightly varying, trends between profiles 3 and 9, i.e. where they are sufficiently far from both jetty and "Rotonda", with the bar trough being 25–40% deeper than the crest. This occurs for all years, except for 2012, when crest and trough depths were very similar ($h_{\mathrm{tr}}/h_{\mathrm{cr}} \cong 1$) as the bar was almost completely destroyed. South of the permeable structure, $h_{\mathrm{tr}}/h_{\mathrm{cr}}$ varies in different ways during the analyzed periods, i.e. it rapidly grows in 2006 and 2013, or remains almost constant in 2010 and 2011. However, it tends to stabilize around 1.4–1.5 at profiles 17–18. Further, the outer bars ($\circ$) do not seem to be strongly influenced by the "Rotonda", as small local changes occur in the crest location between profiles 10 and 12 (Fig. 5a), while the depth ratio slightly increases moving South (Fig. 5b).

Ocean Sci. Discuss., doi:10.5194/os-2016-106, 2017
Manuscript under review for journal Ocean Sci.
Published: 9 January 2017

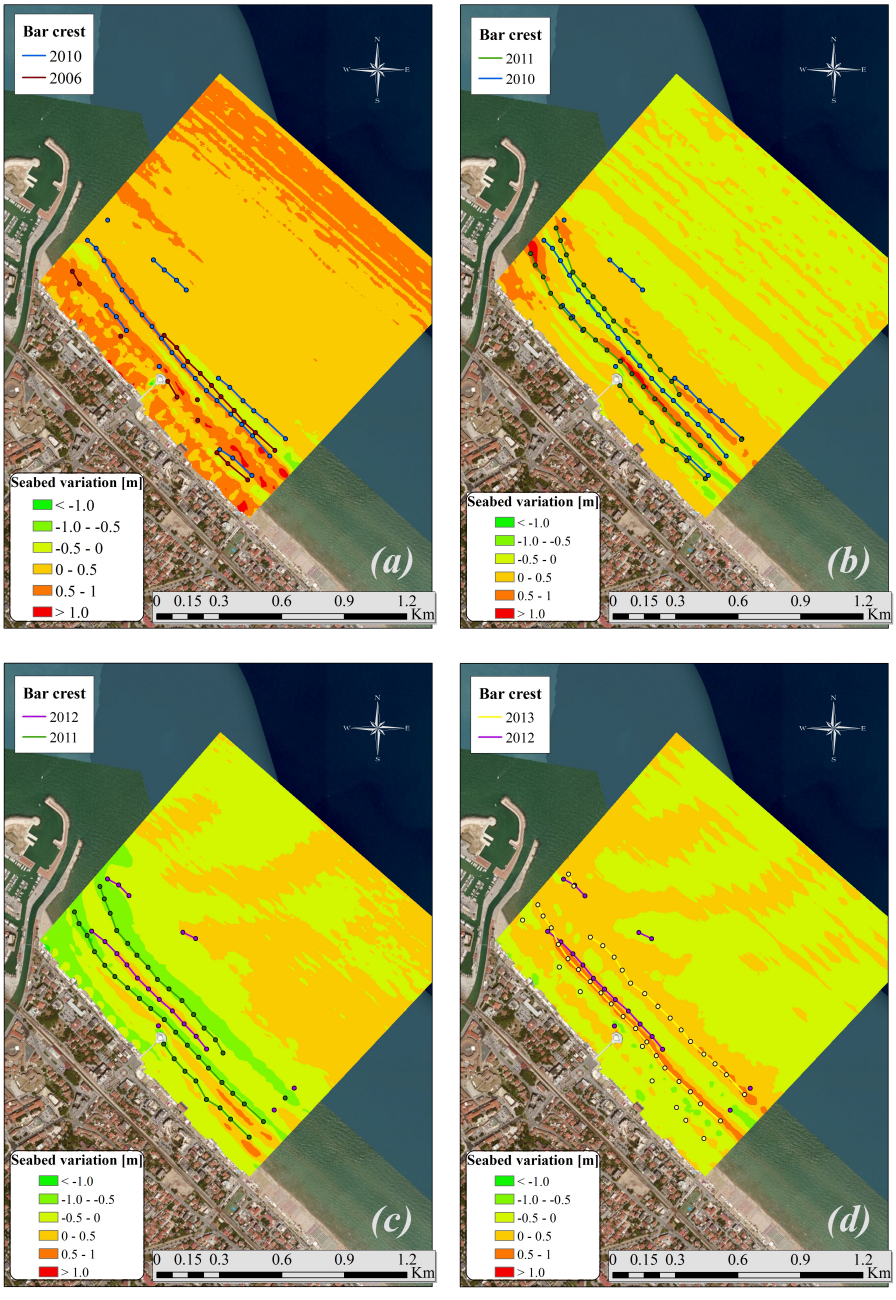

Figure 4. Sea bottom variation within time periods: **(a)** 2006–2010, **(b)** 2010–2011, **(c)** 2011–2012 and **(d)** 2012–2013. Colored lines show the bar-crest locations extracted from the cross-shore profiles.

Ocean Sci. Discuss., doi:10.5194/os-2016-106, 2017
Manuscript under review for journal Ocean Sci.
Published: 9 January 2017

Ocean Science
Discussions
Open Access
EGU

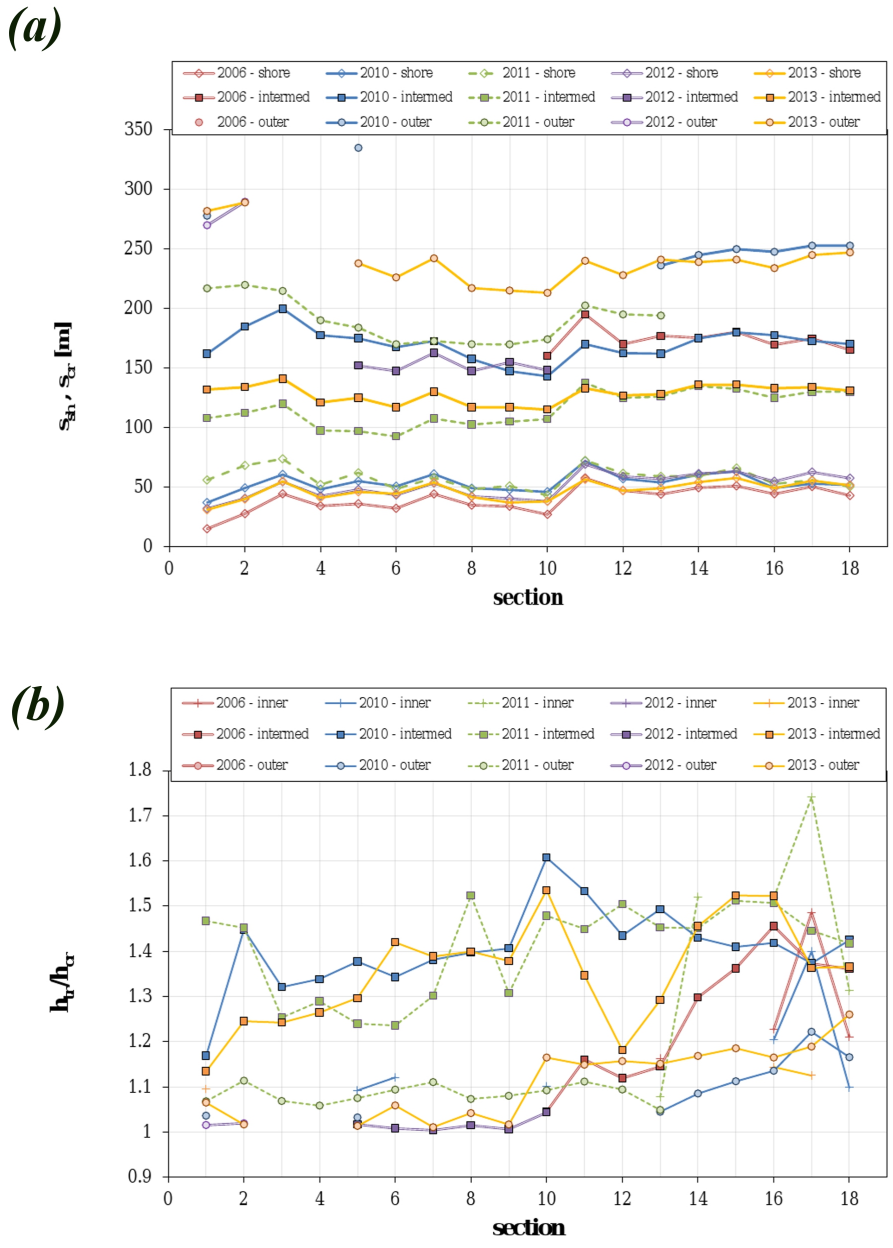

Figure 5. Longshore evolution of bar features: (a) shoreline, middle and offshore bars, (b) ratio between trough and crest depth.

Ocean Sci. Discuss., doi:10.5194/os-2016-106, 2017
Manuscript under review for journal Ocean Sci.
Published: 9 January 2017

4.3 Bar characterization

The previous data have been used to introduce a detailed analysis of the nearshore morphodynamics, especially the bar geometry and migration. Dimensionless parameters are introduced to analyze the bar geometry (e.g., see Grunnet and Ruessink, 2005). In Fig. 6a, the dimensionless bar height $H_{\text{bar}}/h_{\text{cr}}$ is plotted against the dimensionless bar width $W_{\text{bar}}/s_{\text{cr}}$, where the bar dimensions are defined as:

$$H_{\text{bar}} = h_{\text{tr}} - h_{\text{cr}}, \tag{1}$$

$$W_{\text{bar}} = 2(s_{\text{cr}} - s_{\text{tr}}). \tag{2}$$

In general, the bar height seems to increase with the bar width, this occurring for both inner ($+$), middle ($\square$) and outer ($\circ$) bars. Accounting for the surveys referring to 2010, 2011 and 2013, the outer bars are characterized by similar dimensionless heights ($H_{\text{bar}}/h_{\text{cr}}$ ranging between 0 and 0.26), but fairly different widths, the mean $W_{\text{bar}}/x_{\text{cr}}$ being of about 0.17 in 2010, 0.48 in 2011, 0.35 in 2013. The intermediate bars show similar trends, with $H_{\text{bar}}/h_{\text{cr}} = 0.35 - 0.4$ in 2010, 2011 and 2013, and $W_{\text{bar}}/x_{\text{cr}}$ significantly increasing in 2011 (0.54) and 2013 (0.54), with respect to 2010 (0.37). The 2006 middle bar behaves similarly to the 2013 middle bar, while the 2012 bars are always smaller in both height and width, as a consequence of the depth variations occurred in the preceding period. Hence, few and significantly small values referring to 2012 confirm the beach flattening occurred during the 2011–2012 period, dominated by Bora winds, which led to a general beach flattening, as already observed in Figs. 2 and 4c. No significant trends can be obtained from the inner bar data.

The analysis of the longshore distribution of the bar geometry can be undertaken accounting for the bar cross-shore area

$$\Omega = \frac{H_{\text{bar}} W_{\text{bar}}}{2}, \tag{3}$$

which is made dimensionless using both depth and distance to shore of the bar crest.

Figure 6b illustrates that, in general, all bars increase in dimension quite regularly moving southward. Focusing on years 2010, 2011 and 2013, the middle bars increase regularly between profiles 1 and 10, while South of the "Rotonda" (profiles 11–12), the trend is not clear. The outer bars seem not to be affected by the permeable structure and keep increasing moving southward. In 2006 the middle bar generates and starts increasing from profile 10, while in 2012 the trend is unclear, due to the reduced number of sections at which bars occur.

Hence, though Figure 6a illustrates a natural data scattering due to the beach variation both in time and space (e.g., see Grunnet and Ruessink, 2005), a best-fit polynomial curve well represents the geometrical characterization of outer and middle bars of 2010 (blue dashed line) and 2013 (orange dashed line), in both cases giving determination coefficients $R^2 > 0.5$. Further, Figure 6b shows that best-fit curves well reproduce the increasing trend of the outer bars moving southward ($R^2 > 0.75$ for 2010 and 2013, dashed lines), more than that of the middle bars ($R^2 \sim 0.5$, solid lines). The geometrical features of the inshore bars do not offer significant trends.

Ocean Sci. Discuss., doi:10.5194/os-2016-106, 2017
Manuscript under review for journal Ocean Sci.
Published: 9 January 2017

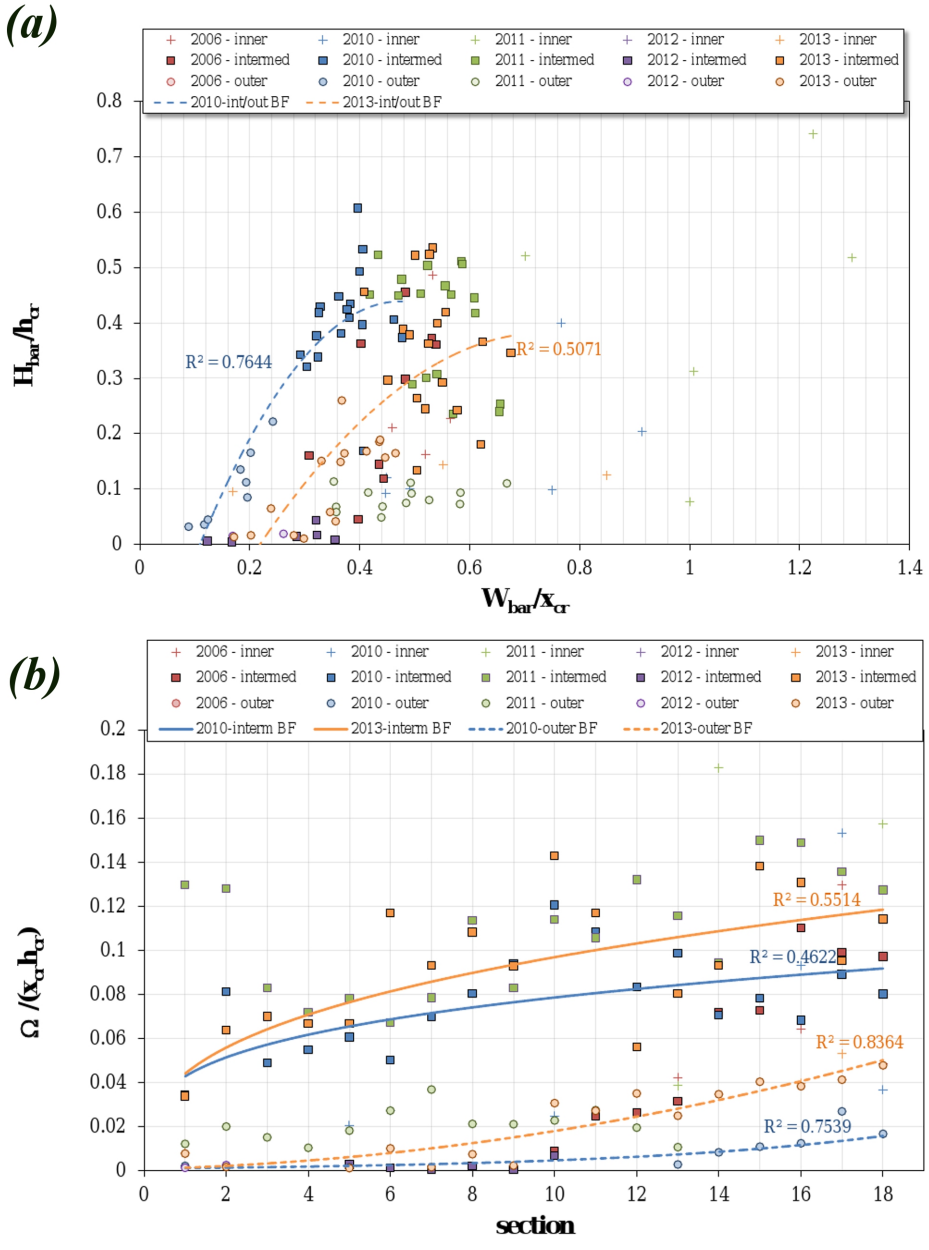

Figure 6. Dimensionless bar features: (a) bar height against bar width, (b) longshore distribution of bar cross-shore area. Dashed and solid lines represent best-fit curves.

Ocean Sci. Discuss., doi:10.5194/os-2016-106, 2017
Manuscript under review for journal Ocean Sci.
Published: 9 January 2017

4.4 Bar dynamics

As suggested by several studies, the generation of subtidal bars may depend on three different mechanisms, i.e. i) breakpoint-related, ii) infragravity-waves-related, and iii) self-organisational mechanisms (e.g., see Wijnberg and Kroon, 2002; Leont'ev, 2011). From the results presented in Sect. 4.1 and 4.3, the bar dynamics in this area might be influenced by either the first or the second mechanism, while the self-organisation seems negligible. In fact, in agreement with Wijnberg and Kroon (2002), such a mechanism cannot explain the bar re-generation between 2012 and 2013 (Fig. 4d), after a general beach smoothing and the partial bar destruction occurred in 2011–2012 (Figs. 2 and 4c).

The destructive nature of the NNE storms significantly affects the bar geometry (beach smoothing), as well as the migration (seaward rather than shoreward), this being strongly influenced by the different wave features (waves coming from NNE were higher and steeper than those coming from ESE), which force the breaking to occur at different locations. Hence, the difference in terms of characteristics of the incoming sea-storm waves directly reflects on the beach morphology, this underlining that the medium-term bar dynamics in the Adriatic sandy beaches are mainly governed by wind waves and breakpoint mechanisms.

Furthermore, steep NNE waves are associated with not excessive storm surges, while less steep ESE waves are associated with larger surges, due to the larger fetch generating in the Adriatic Sea. As an example, two consecutive intense storms occurred in December 2010, the former coming from ESE, the latter from NNE, were characterized by maximum surges of, respectively, 80 and $43\,\mathrm{cm}$, measured within the protected basin of the Ancona harbor (data from Rete Mareografica Nazionale, ISPRA, http://www.mareografico.it). This leads to larger water depths over the crest (h_{cr}) and smaller relative wave heights (H/h_{cr}) during ESE than during NNE waves. In fact, wave propagation from the offshore to the outer bar depth (e.g., using Goda, 2000, who accounts for wave refraction and shoaling) enables one to estimate the local wave inclination (α_l), and also the local wave height $H_{\mathrm{m0},l}$. Then, the actual water depth over the crest during surge may be estimated as $h_{\mathrm{cr,s}} = \overline{h_{\mathrm{cr}}} + \eta_s$, where $\overline{h_{\mathrm{cr}}}$ is the alongshore-averaged still water depth over the crest and η_s the surge contribution, which is different depending on the dominating wave direction, but in agreement with both the data collected at the Ancona harbor (Rete Mareografica Nazionale, ISPRA) and previous literature studies (Orlić et al., 1994; Villatoro et al., 2014).

The above-introduced terms and the relative wave height estimated using the local root-mean-square wave height $H_{\mathrm{rms},l}$ (US Army, 1977), are summarized in Tab. 3. The relative wave height, especially $H_{rms,l}/h_{\mathrm{cr,s}}$, which is larger in 2010–2011 and 2012–2013 and smaller in 2011–2012, suggests, respectively, a landward and seaward bar migration, which has been actually observed (e.g., see Fig. 4). The estimated local wave angles suggest an almost orthogonal-to-shore direction during the NNE-wave-dominated period. Our observations are supported by the numerical results of Dubarbier et al. (2015), who found that the variability in sandbar migration is sensitive to water level over bar crest, this being consistent with storm-surge variations occurring in our site. On the other hand, wave obliquity mainly affects the rates of bar growth and migration, but not their migration direction. This suggests that the difference between Bora and Scirocco waves, in terms of wave incidence, does not influence the bar direction, but eventually their propagation speed.

Ocean Sci. Discuss., doi:10.5194/os-2016-106, 2017
Manuscript under review for journal Ocean Sci.
Published: 9 January 2017

Table 3. Estimate of relative wave height and wave incidence for the examined time periods.

Time range [years]	H_{m0} [m]	$H_{\mathrm{m0},l}$ [m]	$H_{\mathrm{rms},l}$ [m]	$\overline{h_{\mathrm{cr}}}$ [m]	η_s [m]	$h_{\mathrm{cr,s}}$ [m]	$H_{\mathrm{m0},l}/h_{\mathrm{cr,s}}$ [-]	$H_{\mathrm{rms},l}/h_{\mathrm{cr,s}}$ [-]	α_l [°]
2010–2011	1.75	1.51	1.07	2.33	0.60	2.93	0.52	0.36	22
2011–2012	2.25	2.48	1.75	1.81	0.35	2.16	1.15	0.81	5
2012–2013	1.75	1.39	0.98	2.75	0.60	3.35	0.41	0.29	24

5 Discussion

Recent studies on the dynamics of barred beaches suggested us to search for a correlation between wave-climate data, collected by an offshore buoy, and the available bathymetric surveys of an unprotected beach of the Adriatic Sea. Though some results on sandbar migration along the Tyrrhenian Sea were recently illustrated (e.g., Parlagreco et al., 2011), the nearshore bar dynamics of the Adriatic sandy beaches have not been already investigated. However, the correct understanding of the bar migration has a fundamental role in the beach management, also because many Adriatic sandy beaches, like that of Senigallia (see Sect. 2), are characterized by a significant flow of tourism.

Hence, the bathymetric surveys of the area South of the harbor, which has been seen to be stable in the long term, enabled us to analyze a multiple-bar array typical of the sandy beaches of the Middle Adriatic. Such a part of the basin is subject to sea storms mainly due to NNE (Bora) and ESE (Levante-Scirocco) winds, which are characterized by significantly different surges.

The seabed-depth variation and the wave climate between consecutive surveys, as well as the bar features (height, width, location) analyzed for each survey, enabled us to couple the beach/bar dynamics with the wave forcing.

In the studied area the tidal excursion ($\sim 40\,\mathrm{cm}$) is small and only subtidal bars exist. Since the analyzed beach slope ranges between $1:35 \sim 0.03$ (swash zone) and $1:200 \sim 0.005$ (offshore area), such bars fall into the group of two-dimensional longshore bars (Wijnberg and Kroon, 2002). Further, the wave energy in such a microtidal environment is quite high.

In the analyzed region and during the investigated time periods, the beach experienced many sea storms that enabled us to give an overall interpretation to the bar migration process as a function of the wave climate. Coupling wave steepness and the Dean number (i.e. the ratio of wave height to sand fall velocity and wave period), both ESE and NNE are associated with erosive wave conditions (e.g., see Dean and Dalrymple, 2004). However, during the time periods dominated by ESE forcing, waves are characterized by a reduced steepness $H_{\mathrm{m0}}/L_{\mathrm{p0}} = 0.213$ (exactly the same in 2010–2011 and 2012–2013), while this is about $1/3$ larger during the NNE-forcing-dominated period ($H_{\mathrm{m0}}/L_{\mathrm{p0}} = 0.316$). Such a behavior is also confirmed if we do not account for the most energetic waves (see Sect. 4.1), but directly estimate the most frequent combination (H_{m0}, T_{p}). Further, an increase of the bar steepness $H_{\mathrm{bar}}/W_{\mathrm{bar}}$ is associated to a decrease of $H_{\mathrm{m0}}/L_{\mathrm{p0}}$ (e.g., compare the bar geometry in Fig. 2 with the associated wave steepness).

As already stated, steep NNE waves, associated to reduced storm surges, lead to larger relative wave heights $H/h_{cr,s}$, while less steep ESE waves lead to smaller values. As observed by Houser and Greenwood (2005), relative rms heights

Ocean Sci. Discuss., doi:10.5194/os-2016-106, 2017
Manuscript under review for journal Ocean Sci.
Published: 9 January 2017

$H_{\mathrm{rms},l}/h_{cr,s} = 0.3-0.4$ lead to a landward bar migration, associated with bar height increase. This occurs for the outer bar between 2010–2011 ($H_{\mathrm{rms},l}/h_{cr,s} = 0.36$), with a height increase of about 50%, and between 2012–2013 ($H_{\mathrm{rms},l}/h_{cr,s} = 0.29$), when the bar is almost completely regenerated (see also Fig. 2). Conversely, values of $H_{\mathrm{s},l}/h_{cr,s} > 0.6$ lead to a seaward bar migration, as observed in 2011–2012 ($H_{\mathrm{rms},l}/h_{cr,s} = 0.81$), when the outer bar is partially destroyed. Further, waves coming from ESE are characterized by a significant longshore component, due to the large angle between the approaching wave fronts and the coast (see Tab. 3). Differently, waves coming from NNE reach the shore with an almost perpendicular incidence, this improving the intense smoothing of the bars.

Hence, it has been seen that the relative wave height can be properly applied for the prediction of bar migration in an environment different from those already proposed in the literature (e.g., Ruessink and Terwindt, 2000; Houser and Greenwood, 2005), i.e. a nearshore area characterized by a reduced tidal excursion, and partially influenced by the presence of rigid structures. This allows the application of such a predictive parameter for similar nearshore environments, and also for a medium-term prediction. Hence, such a parameter is valid for different environments, characterized by tidal excursions of some centimeters (e.g., Lake Huron, Houser and Greenwood, 2005) to decimeters (Adriatic Sea, present study) to meters (e.g., North Sea, Ruessink and Terwindt, 2000). Assuming that the bar migration mainly occurs during sea storms, the involved sediment transport mainly depends on the incoming short waves (especially when the bars move landward, i.e. ESE waves dominating) and the undertow (especially for seaward motion, associated with NNE waves), with the infragravity waves probably being of some importance in such a dissipative beach (e.g., see Wright and Short, 1984; Ruessink et al., 1998).

While the correlation between bar width and bar height is clear only for some cases, the former increasing with the latter, an overview of the available data enable further conclusions. Between 2010 and 2011, the largest waves, mainly propagating from ESE, provided a height increase of the outer bar (in agreement with Houser and Greenwood, 2005) only North of the "Rotonda", and, at the same time, a width increase and a steepness reduction of both outer and intermediate bars (blue and green symbols in Fig. 6a). While between 2011 and 2012 the bars are largely smoothed due to the NNE dominating waves (purple symbols), the ESE stormy conditions occurred between 2012 and 2013 gave rise to geometric features of the bars similar to those observed in 2011 (orange symbols).

The cross-shore bar area increases moving southward, especially from the Senigallia harbor to the "Rotonda", which partially disturbs the growth of the middle bar. This could also be analyzed in view of the equilibrium-profile theory (Dean, 1991), which describes the long-term beach equilibrium of a natural beach, i.e. the balance between erosive and accretive forcing, through:

$$h = Ax^{2/3}, \tag{4}$$

where h is the water depth and x the distance to shoreline. A is a dimensional shape parameter, directly related to the median grain diameter d_{50} (Hanson and Kraus, 1989). Though recent models account for further parameters, like seasonal changes (Inman et al., 1993) or the generation of submerged bars (Holman et al., 2014), their application is fairly difficult and it has been demonstrated that Eq. 4 properly represents the long-term natural profile, to be used for coastal engineering purposes (e.g., Walton and Dean, 2007; Soldini et al., 2013). From the analysis of such equilibrium profiles, it can be observed that d_{50} slightly decreases moving southward, in agreement with the sediment-size distribution observed in 1989 and 1990 by

Ocean Sci. Discuss., doi:10.5194/os-2016-106, 2017
Manuscript under review for journal Ocean Sci.
Published: 9 January 2017

Lorenzoni et al. (1998a). This is probably due to: i) the river jetty (Fig. 1a), which induces a complex flow field, i.e. a mix of refraction, diffraction and reflection, that generates wave-wave interactions, crossing waves and intense vorticity, especially when sea storms come from ESE (e.g., see Postacchini et al., 2014); ii) the river discharge, especially during severe weather conditions, which gives rise to an intense plume that both propagates southeastward and promotes sediment deposition along its path (e.g., see Brocchini et al., 2016). Hence, the dynamics induced by such phenomena suggest both a deposition of larger sediments immediately south of the jetty, where a more turbulent flow field exists, and a mobilization of finer sands coupled with their transport far from the jetty.

The similar geometry of the bars (width, height, steepness, cross-shore area) in 2011 and 2013, hence suggests that similar medium-term wave features (direction, height, period in 2010-2011 and 2012-2013, respectively) provide similar beach responses, while the initial morphological conditions, respectively represented by the 2010 and 2012 surveys, though significantly different, slightly affect the beach evolution. Further, permeable and impermeable structures locally affect the dynamics of the submerged bars, but do not change their migration direction and their macroscopic features, which are thus dominated by the dominant wave forcing.

6 Conclusions

The nearshore dynamics is characterized by different levels of analysis: long-period (i.e. order of decades) beach stability, medium-term (i.e. order of years or seasons) evolution of the main beach forms (e.g., submerged bars, artificial nourishments) and short-term (i.e. order of days or hours) erosion of the beach profile. While long- and short-term dynamics have been widely investigated, this is not the case for the medium-term beach variability. However, the recent findings on the main processes occurring in the nearshore region suggested us to investigate the medium-term morphodynamics of a sandy barred beach, i.e. that of Senigallia, in the Middle Adriatic Sea.

The present work both illustrates how a proper buoy-data handling leads to the prediction of the morphological changes of a barred beach and offers a useful tool, for coastal engineers and managers, to: i) properly predict the emerged beach stability (e.g., shoreline retreat, erosion), ii) accurately design nourishments for submerged beach recovery, iii) estimate the sediment transport flux through the entrance of nearby harbors, iv) choose the best place to drop the dredged sediment coming from nearby harbors, eventually with nourishment purposes.

A more detailed analysis could be achieved through use of either data collected by another waverider (e.g., that of Cesenatico, FC, which is $\sim 80\,\mathrm{km}$ North of Senigallia) or a reconstructed climate (e.g., Mentaschi et al., 2015) to characterize the wave forcing in the period 2006–2010. Further, the dynamics of the nearshore area before, during and after storm events could also be inspected by means of novel devices like: i) Lagrangian drifters, able at measuring both three-dimensional hydrodynamics and seabed depth (e.g., Postacchini et al., 2016a), ii) video-monitoring systems, to reconstruct the wave field and bed morphology (e.g., Palmsten et al., 2015), available at the Senigallia harbor since July–August 2015, iii) radar images, like those used for the reconstruction of both wave field and bathymetry, through the depth inversion technique (e.g., Ludeno et al., 2015).

Ocean Sci. Discuss., doi:10.5194/os-2016-106, 2017
Manuscript under review for journal Ocean Sci.
Published: 9 January 2017

References

Aagaard, T., and Greenwood, B.: Suspended sediment transport and the role of infragravity waves in a barred surf zone. Mar. Geol., 118(1), 23–48, 1994.

Aagaard, T., Davidson-Arnott, R., Greenwood, B., and Nielsen, J.: Sediment supply from shoreface to dunes: linking sediment transport measurements and long-term morphological evolution, Geomorphology, 60, 205–224, 2004.

Alsina, J. M., Cáceres, I., Brocchini, M., and Baldock, T. E.: An experimental study on sediment transport and bed evolution under different swash zone morphological conditions, Coast. Eng., 68, 31–43, 2012.

Alsina, J. M., Padilla, E. M., Cáceres, I.: Sediment transport and beach profile evolution induced by bi-chromatic wave groups with different group periods, Coast. Eng., 114, 325–340, 2016.

Baldock, T. E., Manoonvoravong, P., and Pham, K. S.: Beachface morphology and surf beat sediment transport in laboratory scale surf and swash zones, J. Coastal Res., SI 50, 631–635, 2007.

Benavente, J., Río, L. D., Gracia, F., and del Pozo, J. M.: Coastal flooding hazard related to storms and coastal evolution in Valdelagrana spit (Cadiz Bay Natural Park, SW Spain), Cont. Shelf Res., 26, 1061–1076, 2006.

Brocchini, M., Calantoni, J., Reed, A. H., Postacchini, M., Lorenzoni, C., Russo, A., Mancinelli, A., Corvaro, S., Moriconi, G., and Soldini, L.: Summertime conditions of a muddy estuarine environment: the EsCoSed project contribution, Water Sci. Technol., 71, 1451–1457, 2015.

Brocchini, M., Calantoni, J., Postacchini, M., Sheremet, A., Staples, T., Smith, J., Reed, A. H., Braithwaite, E. F., Lorenzoni, C., Russo, A., Corvaro, S., Mancinelli, A., and Soldini, L.: Comparison between the wintertime and summertime dynamics of the Misa River estuary, Mar. Geol., in press, 2016.

Dean, R. G.: Equilibrium beach profiles: characteristics and applications, J. Coastal Res., 7, 53–84, 1991.

Dean, R. G. and Dalrymple, R. A.: Coastal Processes with Engineering Applications, Cambridge University Press, Cambridge, UK , 2004.

Dubarbier, B., Castelle, B., Marieu, V., and Ruessink, G.: Process-based modeling of cross-shore sandbar behavior, Coast. Eng., 95, 35-50, 2015.

Gallagher, E. L., Elgar, S., and Guza, R. T.: Observations of sand bar evolution on a natural beach, J. Geophys. Res.-Oceans, 103(C2), 3203–3215, 1998.

Goda, Y.: Random seas and design of marine structures, Advanced series on ocean engineering vol. 15, World Scientific, Singapore, 2000.

Goulart, E. S., and Calliari, L. J.: Medium-term morphodynamic behavior of a multiple sand bar beach, J. Coastal Res., SI 65(2), 1774–1779, 2013.

Grunnet, N. M., and Ruessink, B. G.: Morphodynamic response of nearshore bars to a shoreface nourishment, Coast. Eng., 52(2), 119-137, 2005.

Hanson, H. and Kraus, N. C.: GENESIS: Generalized Model for Simulating Shoreline Change, Report 1, Technical Reference, Tech. rep., Coastal Engineering Research Center, Vicksburg, MS, USA, DTIC Document, 1989.

Holman, R. A., Lalejini, D. M., Edwards, K., and Veeramony, J.: A parametric model for barred equilibrium beach profiles, Coast. Eng., 90, 85–94, 2014.

Houghton, K., Vafeidis, A., Neumann, B., and Proelss, A.: Maritime boundaries in a rising sea, Nat. Geosci., 3, 813–816, 2010.

Houser, C. and Greenwood, B.: Profile response of a lacustrine multiple barred nearshore to a sequence of storm events, Geomorphology, 69, 118–137, 2005.

Ocean Sci. Discuss., doi:10.5194/os-2016-106, 2017
Manuscript under review for journal Ocean Sci.
Published: 9 January 2017

Inman, D. L., Elwany, M. H. S., and Jenkins, S. A.: Shorerise and bar-berm profiles on ocean beaches, J. Geophys. Res.-Oceans, 98, 18181–18199, 1993.

Kuriyama, Y., and Nakatsukasa, T.: A one-dimensional model for undertow and longshore current on a barred beach, Coast. Eng., 40(1), 39–58, 2000.

Leont'ev, I.: Submarine bars on sandy coasts, Oceanology+, 51, 141–147, 2011.

Lippmann, T. C. and Holman, R. A.: The spatial and temporal variability of sand bar morphology, J. Geophys. Res.-Oceans, 95, 11575-11590, 1990.

Lorenzoni, C., Mancinelli, A., and Soldini, L.: Caratteristiche sedimentologiche del litorale a Nord di Ancona. Analisi del movimento delle ghiaie (in Italian), in: Atti dell'Istituto di Idraulica dell'Università di Ancona, Università di Ancona, Ancona, p. 54, 1998a.

Lorenzoni, C., Mancinelli, A., and Soldini, L.: Evoluzione batimetrica del litorale a nord di Ancona. Analisi del trasporto solido trasversale (in Italian), in: Atti dell'Istituto di Idraulica dell'Università di Ancona, Università di Ancona, Ancona, p. 46, 1998b.

Lorenzoni, C., Postacchini, M., Brocchini, M., and Mancinelli, A.: Experimental study of the short-term efficiency of different breakwater configurations on beach protection, Journal of Ocean Engineering and Marine Energy, 2(2), 195–210, 2016.

Ludeno, G., Reale, F., Dentale, F., Pugliese Carratelli, E., Natale, A., Soldovieri, F., and Serafino, F.: An X-Band Radar System for Bathymetry and Wave Field Analysis in a Harbour Area, Sensors, 15(1), 1691–1707, 2015.

Mentaschi, L., Besio, G., Cassola, F., and Mazzino, A.: Performance evaluation of Wavewatch III in the Mediterranean Sea, Ocean Model., 90, 82–94, 2015.

Orlić, M., Kuzmić, M., and Pasarić, Z.: Response of the Adriatic Sea to the bora and sirocco forcing, Cont. Shelf Res., 14(1), 91–116, 1994. (2015). . Water Resources Research, 51(9), 7238-7257.

Palmsten, M. L., Kozarek, J. L., and Calantoni, J.: Video observations of bed form morphodynamics in a meander bend, Water Resources Res., 51(9), 7238–7257, 2015.

Parlagreco, L., Archetti, R., Simeoni, U., Devoti, S., Valentini, A., and Silenzi, S.: Video-monitoring of a barred nourished beach (Latium, Central Italy), J. Coastal Res., SI 64, 110–114, 2011.

Plant, N. G., Holland, K. T., Puleo, J. A., and Gallagher, E. L.: Prediction skill of nearshore profile evolution models. J. Geophys. Res.-Oceans, 109(C1), 2004.

Postacchini, M., and Brocchini, M.: A wave-by-wave analysis for the evaluation of the breaking-wave celerity, Appl. Ocean Res., 46, 15–27, 2014.

Postacchini, M., Brocchini, M., and Soldini, L.: Vorticity generation due to cross-sea, J. Fluid Mech., 744, 286–309, 2014.

Postacchini, M., Centurioni, L. R., Braasch, L., Brocchini, M., and Vicinanza, D.: Lagrangian Observations of Waves and Currents From the River Drifter, 41(1), 94–104, doi:10.1109/JOE.2015.2418171, 2016a.

Postacchini, M., Russo, A., Carniel, S., and Brocchini, M.: Assessing the hydro-morphodynamic response of a beach protected by detached, impermeable, submerged breakwaters: a numerical approach, J. Coastal Res., 32(3), 590–602, 2016b.

Ranasinghe, R., Duong, T., Uhlenbrook, S., Roelvink, D., and Stive, M.: Climate-change impact assessment for inlet-interrupted coastlines, Nat. Clim. Chang., 3, 83–87, 2013.

Ruessink, B. G., Houwman, K. T. and Hoekstra, P.: The systematic contribution of transporting mechanisms to the cross-shore sediment transport in water depths of 3 to 9 m, Mar. Geol., 152(4), 295–324, 1998.

Ruessink, B. and Terwindt, J.: The behaviour of nearshore bars on the time scale of years: a conceptual model, Mar. Geol., 163, 289–302, 2000.

Ocean Sci. Discuss., doi:10.5194/os-2016-106, 2017
Manuscript under review for journal Ocean Sci.
Published: 9 January 2017

Ruggiero, P., Walstra, D. J. R., Gelfenbaum, G., and van Ormondt, M.: Seasonal-scale nearshore morphological evolution: Field observations and numerical modeling, Coast. Eng., 56(11), 1153–1172, 2009.

Soldini, L., Antuono, M., and Brocchini, M.: Numerical modeling of the influence of the beach profile on wave run-up, J. Waterw. Port C.-ASCE, 139, 61–71, 2013.

Soldini, L., Lorenzoni, C., Brocchini, M., Mancinelli, A., and Cappietti, L.: Modeling of the wave setup inshore of an array of submerged breakwaters, J. Waterw. Port C.-ASCE, 135(2), 38–51, 2009.

US Army, Corps of Engineers: Coastal Engineering Research Center: Shore Protection Manual, Coastal Eng. Res. Center, Fort Belvoir, VA, 1977.

Villatoro, M., Silva, R., Méndez, F. J., Zanuttigh, B., Pan, S., Trifonova, E., Losada, I. J., Izaguirre, C., Simmonds, D., Reeve, D. E., Mendoza, E., Martinelli, L., Formentin, S. M., Galiatsatou, P., and Eftimova, P.: An approach to assess flooding and erosion risk for open beaches in a changing climate, Coast. Eng., 87, 50–76, 2014.

Walton, T. and Dean, R.: Temporal and spatial change in equilibrium beach profiles from the Florida Panhandle, J. Waterw. Port C.-ASCE, 133, 364–376, 2007.

Wijnberg, K. M. and Kroon, A.: Barred beaches, Geomorphology, 48, 103–120, 2002.

Wright, L. D. and Short, A. D.: Morphodynamic variability of surf zones and beaches: a synthesis, Mar. Geol., 56(1), 93–118, 1984.